Giant Anisotropic Magnetoresistance and Excess Resistivity in Amorphous $U_{1-x}Sb_x$ Ferromagnets

P. P. Freitas
Centro de Física da Matéria Condensada, Instituto Nacional de Investigação Científico, Av. Prof. Gama Pinto 2, 1699, Lisbon, Portugal and Instituto de Engenharia de Sistemas e Computadores, Redol 9-3, 1000 Lisbon, Portugal

T. S. Plaskett
IBM Research Division, T. J. Watson Research Center, P.O. Box 218, Yorktown Heights, New York 10598
(Received 2 January 1990)

$U_{1-x}Sb_x$ amorphous ferromagnets were prepared that show a magnetoresistance anisotropy (AMR) reaching 26% at 10 K, in a 50-kOe field. This is a striking result, since the AMR of typical amorphous ferromagnets does not exceed 1%. Large excess resistivity caused by domain walls is found to scale with β'^2, where β' is the tangent of the Hall angle.

PACS numbers: 75.50.Kj, 72.15.Gd

This Letter describes transport and magnetic properties of a new class of amorphous ferromagnets showing a 26% magnetoresistance anisotropy at saturation and at low temperature. This is a striking result since typical amorphous ferromagnets have magnetoresistance anisotropies not in excess of 1% at best.[1,2] This quantity is defined as $(\rho_{\parallel}-\rho_{\perp})/\rho_0$, where $\rho_{\parallel}$ and $\rho_{\perp}$ are the resistivities at saturation when the magnetization is parallel or perpendicular to the current direction, and $\rho_0=\frac{1}{3}\rho_{\parallel}+\frac{2}{3}\rho_{\perp}$. Our results also show large excess resistivity at $\pm H_c$ when the field is applied perpendicular to the current, where H_c is the coercive field. This excess resistivity is caused by the distortion of current lines by domain walls and scales with the square of the tangent of the Hall angle.[3,4]

Crystalline USb and U_3Sb_4 compounds order antiferromagnetically ($T_N=213$ K) and ferromagnetically ($T_c=146$ K), respectively.[5] All the Th_3P_4 compounds (U_3Sb_4, U_3P_4, and U_3As_4) show anomalously large Hall angles,[6] Kerr rotations,[7] and resistivity and magnetoresistance anisotropies.[8] The $5f$ electrons are responsible for the U magnetic moment, that reaches $1.8\mu_B$ in U_3Sb_4, while p-f and d-f hybridization plays a role in the highly anisotropic nature of the magnetic and transport properties.

Amorphous $U_{1-x}Sb_x$ films were prepared by dc magnetron sputtering following our quest for amorphous U systems where the U is optically and magnetically active.[9-11] The films are 2000 Å thick and are overcoated with a 400-Å SiO_2 passivation layer. Sample composition was checked by wet-chemical analysis. X-ray data show the films to be amorphous, with none of the Bragg peaks correspondent to U_3Sb_4 and USb polycrystalline material (inset of Fig. 1). The U-U distances in the amorphous sample cannot be determined from our data alone. However, and as we shall see, the magnetic properties of these amorphous films are similar to those of crystalline U_3Sb_4. This means that short-range order creates an environment where the U-U distances in the amorphous material are comparable to those found in the close-packed Th_3P_4 type of body-centered cubic crystal structure characteristic of U_3Sb_4 compounds. In this case the U-U distance is 4.25 Å. According to the Hill plot,[12] it is this distance that determines the existence of a magnetic moment in the U atom.

Three a-$U_{1-x}Sb_x$ samples were prepared with compositions $x=0.37$, 0.55, and 0.64 and with Curie temperatures of 98, 132, and 90 K, respectively. Sample composition was checked by wet-chemical analysis. The magnetic moment per U atom has a lower bound of $1.2\mu_B$ for

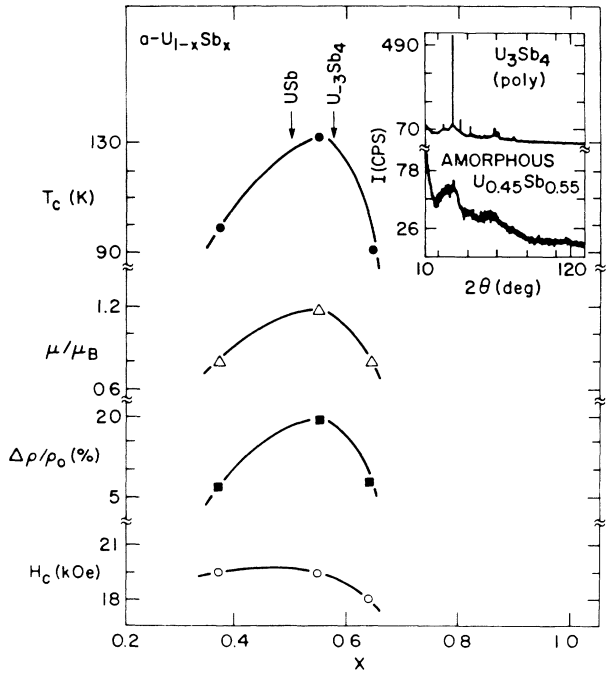

FIG. 1. Composition dependence of T_c, μ/μ_B, $\Delta\rho/\rho_0$ (15 K, 20 kOe), and H_c (15 K) for a-$U_{1-x}Sb_x$ films. Inset: Typical x-ray diffractograms for polycrystalline and amorphous films.

$x=0.55$ and decreases to $0.8\mu_B$ for $x=0.37$ and 0.64. Notice that the $x=0.55$ sample has a Curie temperature and a magnetic moment close to those quoted for crystalline U_3Sb_4 ($x=0.56$). Ferromagnetism is still observed for $x=0.37$ and 0.64 while the crystalline USb compound ($x=0.5$) is already antiferromagnetic. In all the amorphous samples studied, the magnetic moment was found to lay in the plane of the sample. The composition dependences of the Curie temperature, the magnetic moment, the anisotropic magnetoresistance, and the coercive field are shown in Fig. 1. All samples show large Hall angles reaching 20° at low temperature, values similar to those reported for the crystalline compounds.[6]

The magnetization hysteresis loop for a a-$U_{0.45}Sb_{0.55}$ film measured at 15 K in a SQUID magnetometer is shown in Fig. 2. The field is applied in the plane of the sample. Because of the large coercive field H_c the data indicate only a lower bound for the magnetic moment, the real saturation value being probably higher. Measurements up to higher fields will be needed to determine the relative strength of local anisotropy and exchange fields. The coercive field H_c has a thermally activated temperature dependence similar to that found for amorphous Tb-Fe ferromagnets,[13]

$$H_c=3K/M_s-\alpha' T^{1/2}. \tag{1}$$

Here K is the local anisotropy constant, M_s is the magnetization of a characteristic spin-flipping volume, and α' is a constant. The overall functional dependence predicted by Eq. (1) does represent the data reasonably well up to 50 K (see dashed line, inset of Fig. 2). Another feature of the low-temperature magnetization of these materials is its dependence on the field-cooling or zero-field-cooling process. This is similar to what is found in spin glasses and random ferromagnets.

Transport properties were measured on rectangular samples typically 10 mm long, 2–3 mm wide, and 2000 Å thick. Collinear contacts were used and care was taken to avoid sample crystallization upon contact preparation. Sample resistivity at 10 K ranges from 281 to 558 $\mu\Omega$ cm for $0.36<x<0.65$, respectively. These values are quite high even for an amorphous material, and are caused by the large effective masses of $6d$ and $5p$ conduction electrons. This is also the reason for the large resistivities found in the crystalline USb and U_3Sb_4 compounds.[5] Magnetoresistance measurements were done at 15 K in a continuous-flow cryostat and using an electromagnet (0–20 kOe). One of the samples was measured in a superconducting magnet in fields up to 60 kOe, to compare magnetoresistance and magnetization hysteresis cycles.

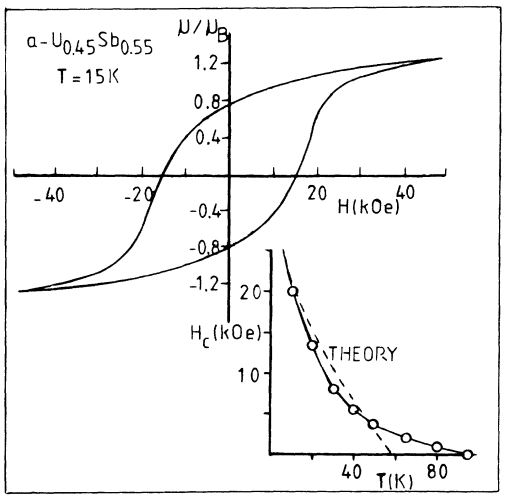

FIG. 2. Magnetization hysteresis cycle at 15 K. Inset: The temperature dependence of the coercive field.

The resistivity of ferromagnets can be written as a sum of an isotropic spin-disorder term $\rho_{sd}=\rho_{dis}-\alpha m_l^2$ and an anisotropic term related to the spin-orbit interaction $\rho_{ani}=-\beta m_\perp^2$. Here ρ_{dis} is the magnetic resistivity well above T_c, m_l is the moment averaged over the mean-free-path distance, $m_\perp$ is the component of m_l perpendicular to the current direction, and α and β are constants.

$$\rho=\rho_{dis}-\alpha m_l^2-\beta m_\perp^2. \tag{2}$$

The $-\beta\ldots$ term describes the magnetization rotation with respect to the current direction, and is responsible for the resistivity anisotropy at saturation. This term predicts maxima in $\rho_\perp$ at $\pm H_c$ when magnetization reversal occurs through rotation processes. The $-\alpha\ldots$ term is isotropic and reflects the spin correlations between U atoms on neighbor sites. Its behavior has been described in detail by Senoussi[14] for Ni-Mn spin glasses.

A third mechanism leading to low-field magnetoresistance in crystalline or amorphous ferromagnets was introduced by Berger.[3,4] He showed that current lines are distorted by twice the Hall angle at 180° domain walls oriented perpendicular to the current direction. This gives rise to excess Ohmic resistivity at H_c, $\Delta\rho/\rho_s$, scaling with β'^2, where β' is the tangent of the Hall angle and ρ_s is the $\rho_\perp$ value at saturation (no walls),

$$\Delta\rho/\rho_s=C\beta'^2. \tag{3}$$

C is a constant of order unity depending on the wall configuration. Equation (3) assumes that the wall spacing is much smaller than the sample width. This mechanism leads to peaks in $\rho_\perp$ at the coercive field caused by the distortion of the current lines by the walls.

Figure 3 shows the resistance behavior versus applied field, at 10 K, for the $x=0.55$ sample. The data were taken with the field applied in the plane of the sample either parallel or perpendicular to the current. First, notice the giant resistance anisotropy observed at saturation and at this temperature, with

$$\Delta\rho/\rho_0=(\rho_\parallel-\rho_\perp)/\rho_0=26\%. \tag{4}$$

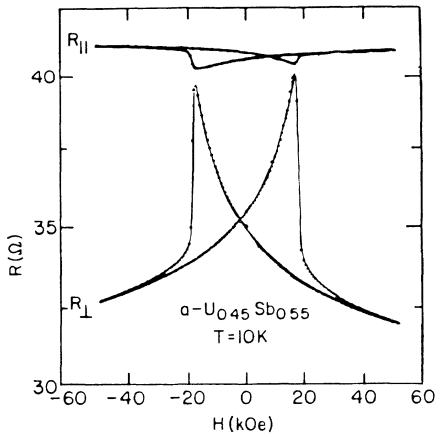

FIG. 3. Magnetoresistance at 10 K, for fields applied in the plane of the sample, either parallel or perpendicular to the current. Notice the 26% resistivity anisotropy at saturation and the large excess resistivity in $\rho_\perp$ at $\pm H_c$.

This means that $\beta \gg \alpha$ in these systems. This resistance anisotropy at saturation exceeds by far typical values found for transition-metal[1] and rare-earth containing amorphous ferromagnets.[2]

Second, notice the sharp peaks of $\rho_\perp$ at $\pm H_c$. These may correspond to the large excess resistivity predicted by Eq. (3) since these samples have very large Hall angles with $\beta' \approx 0.13$. Third, but not least important, notice that there is only a slight variation in $\rho_\parallel$ during magnetization reversal.

Let us start with the $\rho_\parallel$ data. The upper curve in Fig. 3 shows that $\rho_\parallel$ never departs more than 1.5% from its saturation value during magnetization reversal. This is to be compared to a 26% decrease in the saturation resistivity when the magnetization becomes perpendicular to the current. We conclude that it is energetically favorable for magnetization reversal to proceed mainly through domain-wall displacement, with the net magnetization direction induced by the applied field. The observed 1.5% change of $\rho_\parallel$ as the field is decreased from saturation towards H_c corresponds to the increase in dispersion of the moments around the field direction. This is reflected by the $-\beta m_\perp^2$ term in Eq. (2). In this case the current distortion mechanism will not contribute since domain walls are essentially parallel to the current.

Consider now the $\rho_\perp$ curve. The net magnetization is now perpendicular to the current. This leads to domains with walls perpendicular to the current, and then the two sharp peaks observed at $\pm H_c$ can be caused either by current distortion at domain walls or by the anisotropic $-\beta m_\perp^2$ term. Since the magnetization reversal occurs mainly through domain-wall motion as concluded above, the anisotropic term should give only a slight 1%–2% increase in $\rho_\perp$ over the magnetization reversal process. This cannot explain the 23% increase in $\rho_\perp$ at $\pm H_c$ compared to the $\rho_\perp$ saturation value. This leaves Eq. (3)

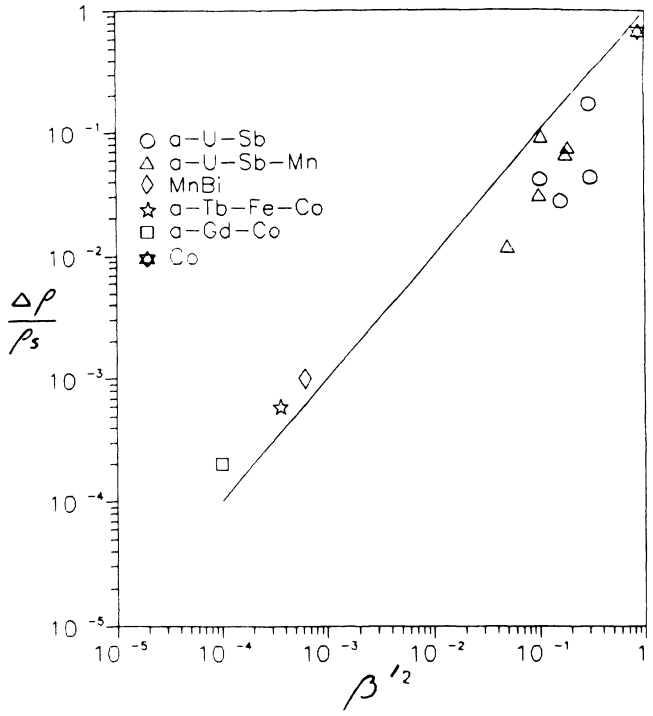

FIG. 4. Plot of the excess resistivity $\Delta\rho/\rho_s$ at H_c vs the β'^2, where β' is the tangent of the Hall angle for different types of systems. The solid line corresponds to Eq. (3) with $C=1$.

and the current distortion model as a good candidate to explain the sharp peaks of $\rho_\perp$ observed at $\pm H_c$.

In Fig. 4 we plot $\Delta\rho/\rho_s$ vs β'^2 for all our amorphous $U_{1-x}Sb_x$ samples. For comparison, we added data for a-U-Sb-Mn,[15] a-Gd-Co,[3] a-Tb-Fe-Co,[16] crystalline MnBi films,[3] and bulk Co at 4.2 K.[17] The solid line corresponds to Eq. (3) with $C=1$. We find a remarkable scaling of $\Delta\rho/\rho_s$ with β'^2 over 4 orders of magnitude in all these different systems. This shows that this mechanism involving the distortion of current lines by walls is probably responsible for the large excess resistivities found for $\rho_\perp$ in the a-$U_{1-x}Sb_x$ systems. Direct domain observation was made in crystalline U_3As_4. From crystal field and exchange constant parameters the wall thickness was predicted to be a few angstrom.[18]

Having explained the nature of the large excess resistivity in the perpendicular resistivity, we are still left with an intriguing phenomena, the large resistivity anisotropy at saturation.

Henkie[6] has also found large anisotropic magnetoresistance in U_3As_4 single crystals. He distinguished a large contribution coming from the anisotropic resistivity of a single domain for different magnetization orientations with respect to the current direction. He also described a small excess resistivity caused by domain walls. He proposed p-f anisotropic mixing as the cause of the single-domain resistivity anisotropy but no theory was presented.

Consider now the anisotropic magnetoresistance caused by an anisotropic scattering cross section. In this case different resistivity values at saturation are obtained, depending on the angle between the magnetization and the current. This effect has been discussed in detail for $3d$ transition metals and $4f$ rare earths. For localized moments in amorphous rare earths the magnetoresistance anisotropy arises from the quadrupole spin polarization.[19] This model also involves the hybridization of the $5d$ states with the conduction electrons. As the $5d$ admixed states lie close to the $4f$ shell they feel strongly the orbital anisotropy of this shell. This feature can be compared with p-f mixing in the actinides. The temperature and field dependences of the magnetoresistance depend on the crystal-field splitting for the rare-earth ions. Typical $\Delta\rho/\rho_0$ values are in the 10^{-3}-10^{-4} range. This model fails, however, to give an explanation for the observed anisotropic magnetoresistance of the $U_{1-x}Sb_x$ films. First, the magnetoresistance values observed seem too large to be accounted for by this model. Second, but not least important, all samples show comparable coercive fields at low temperature, and therefore similar local crystal fields [see Eq. (1)]. According to this model the magnetoresistance anisotropy should then be similar for all samples. On the contrary, we observe a pronounced maximum of the magnetoresistance for the $x=0.55$ sample, where T_c and the magnetic moments are larger.

The light actinides can also be viewed as transitionlike metals with hybridized $5f$-$6d$ narrow bands superimposed on a broad $7s$ conduction band. For $3d$ transition metals, and due to the spin-orbit interaction, the cross section for electron scattering by impurities depends on the angle between the magnetization and the current directions. Using this model, Jaoul, Campbell, and Fert derived[20]

$$\Delta\rho/\rho_0=\gamma(\rho_\downarrow/\rho_\uparrow-1)\,, \tag{5}$$

where $\gamma=\{(V_{so}^{\parallel})^2-(V_{so}^{\perp})^2\}/\Delta^2$. Here V_{so} is a matrix element of the spin-orbit interaction and Δ is the exchange splitting energy. We see that in order to have large $\Delta\rho/\rho_0$ values $\rho_\uparrow$ must be small which means that the spin-up Fermi level is almost outside the spin-up band. According to photoemission data, this is the case in USb (Ref. 21) and U_3Sb_4 (Ref. 22) materials $[D_\uparrow^{d\text{-}f}(E_F)\ll D_\downarrow^{f}(E_F)]$. This mechanism can lead to $\Delta\rho/\rho_0$ values of the order of 10^{-2}-10^{-1} such as those found in the transition-metal alloys, and of the order of those we find in the $U_{1-x}Sb_x$ amorphous films. Two conditions were, however, used to derive Eq. (5) that may not be fulfilled. First, the spin-orbit interaction was used in perturbation theory to determine the perturbed spin-up and spin-down wave functions. Second, the two spin subbands were assumed to conduct in parallel (two-current model). The first hypothesis will certainly not work for the $5f$ systems where spin orbit is much larger than in the $3d$ metals. Also, there is no proof for the validity of the two-current model in the $5f$ systems.

This means that the observed giant resistivity anisotropy in these $5f$ amorphous systems cannot be described within existing models. We hope that this work will stimulate theoretical studies leading to the understanding of this phenomena.

We thank T. McGuire, T. Penney, S. von Molnar, R. Gambino, J. M. D. Coey, and L. Berger for helpful comments during different stages of this work.

[1]S. N. Kaul and M. Rosenberg, Phys. Rev. B **27**, 5689 (1983).

[2]A. Fert and R. Azomosa, J. Appl. Phys. **50**, 1886 (1979).

[3]L. Berger, J. Appl. Phys. **49**, 2156 (1978).

[4]A. K. Agarwala and L. Berger, IEEE Trans. Magn. **22**, 544 (1986).

[5]J. Fournier and R. Troc, in *Handbook on the Physics and Chemistry of the Actinides,* edited by A. J. Freeman and G. H. Lander (North-Holland, Amsterdam, 1985), p. 29.

[6]Z. Henkie, Bull. Acad. Pol. Sci., Ser. Sci. Chim. **20**, 531 (1972).

[7]W. Reim, J. Schoenes, and P. Wachter, IEEE Trans. Mag. **20**, 1045 (1984).

[8]Z. Henkie, Physica (Amsterdam) **102B**, 329 (1980).

[9]P. P. Freitas, T. S. Plaskett, and T. R. McGuire, J. Appl. Phys. **63**, 3746 (1988).

[10]P. P. Freitas, T. S. Plaskett, J. M. Moreira, and V. S. Amaral, J. Appl. Phys. **64**, 5453 (1988).

[11]P. P. Freitas, T. S. Plaskett, and M. M. Godinho, J. Phys. (Paris) Colloq. **49**, C8-1357 (1988).

[12]H. H. Hill, in *Plutonium 1970 and other Actinides,* edited by W. N. Miner (The Metallurgical Society of the AIME, New York, 1970), p. 2.

[13]J. J. Rhyne, J. H. Schelleng, and N. C. Koon, Phys. Rev. B **10**, 4672 (1974).

[14]S. Senoussi, Phys. Rev. Lett. **56**, 2314 (1986).

[15]P. P. Freitas and T. S. Plaskett (to be published).

[16]P. P. Freitas, L. V. Melo, and T. S. Plaskett, in Proceedings of Magnetism and Magnetic Materials-INTERMAG Conference, 1990 (to be published).

[17]V. R. V. Ramanan and L. Berger, J. Appl. Phys. **52**, 2211 (1981).

[18]R. Gemperle, P. Novotny, and A. Menovsky, Phys. Status Solidi **52**, 587 (1979).

[19]A. Fert, R. Azomosa, D. H. Sanchez, and D. Spanjaard, Phys. Rev. B **11**, 5040 (1977).

[20]O. Jaoul, I. A. Campbell, and A. Fert, J. Magn. Magn. Mater. **5**, 23 (1977).

[21]J. Schoenes, Phys. Rep. **66**, 187 (1980).

[22]J. Schoenes, M. Kung, R. Hauert, and Z. Henkie, Solid State Commun. **47**, 23 (1983).